Available online at www.sciencedirect.com
ScienceDirect
Journal of Power Sources 158 (2006) 1195–1201
JOURNAL OF POWER SOURCES
www.elsevier.com/locate/jpowsour

Application of $Pt + RuO_2$ catalysts prepared by thermal decomposition of polymeric precursors to DMFC

L.P.R. Profeti [a], F.C. Simões [a], P. Olivi [a,*], K.B. Kokoh [b], C. Coutanceau [b], J.-M. Léger [b], C. Lamy [b]

[a] *Departamento de Quimica, Faculdade de Filosofia, Ciências e Letras de Ribeirão Preto, Universidade de São Paulo, 14040-901 Ribeirão Preto, SP, Brazil*

[b] *Equipe Electrocatalyse, UMR 6503, CNRS-Universite de Poitiers, 40, Avenue du Recteur Pineau, 86022 Poitiers Cedex, France*

Received 21 July 2005; received in revised form 21 September 2005; accepted 24 September 2005
Available online 28 November 2005

Abstract

Pt-RuO_2 catalysts in the form of pure powder or supported on carbon powder (Vulcan XC72) substrate were prepared by thermal decomposition of polymeric precursors. Catalysts displaying different metal compositions were prepared in order to investigate the influence of catalyst composition. XRD and EDX analyses were employed to determine the composition and crystallinity of the materials. Catalyst morphology was investigated by SEM and TEM. Evaluation of the catalytic activity of the materials toward methanol oxidation was performed in half-cell experiments by cyclic voltammetry and in a single direct methanol fuel cell (DMFC). Electrochemical experiments showed that the catalytic activity of the mixed electrodes toward methanol oxidation is higher than that of Pt alone. Particle dispersion on the carbon substrate and catalyst composition influences their performance toward methanol oxidation. Results indicated a low power density, but the thermal decomposition of polymeric precursors seems to be a promising method to prepare catalysts supported on carbon powder that can be applied to DMFC.

Keywords: Methanol electrooxidation; Fuel cell; Platinum; Ruthenium oxide

1. Introduction

The electrocatalytic oxidation of methanol has been widely investigated not only because methanol is considered to be a model molecule, but also because of the technological interest in its applications in direct methanol fuel cells (DMFC) [1,2].

Energy production from DMFC is very interesting because these fuel cells operate silently and cleanly, which enables their use in electric vehicles, stationary power plants and portable devices [3]. Because of these features, DMFCs are promising candidates to replace H_2 as fuel, mainly in applications where difficulties in handling, transportation, and storage are concerned.

Although the thermodynamic reversible potential for the overall methanol cell reaction (1.214 V) is close to that of the hydrogen fuel cell (1.23 V), DMFC achieves high anodic potential values under operational conditions, yielding lower power density values than those obtained with the H_2 fuel cell [2,4].

The low energy provided by DMFC comes from the slow kinetics of methanol oxidation on the anode, which leads to decreased cell potential [2]. Platinum is the catalyst generally used in the anode. However, when used alone, Pt is poisoned by adsorbed CO species formed in the reaction and its activity is reduced. In order to improve the fuel cell performance, Pt can be combined with other metals, mainly Ru, either as an alloy [5–7] or as ad atoms [8–10]. It is believed that CO species are oxidized by OH species generated at lower potentials on the Ru surface atoms than on Pt [9]. Electronic effects [11] due to the presence of Ru; i.e. changes in the platinum electronic states leading to the weakening of the CO–Pt bond, are also suggested as being an effect due to addition of Ru.

It has been reported that hydrous ruthenium oxides are required for electrodes to achieve high activity toward methanol oxidation. This is because these species can adsorb large

* Corresponding author. Tel.: +55 16 602 3869; fax: +55 16 633 8151.
E-mail address: olivip@ffclrp.usp.br (P. Olivi).

0378-7753/$ – see front matter © 2005 Elsevier B.V. All rights reserved.
doi:10.1016/j.jpowsour.2005.09.061

quantities of OH species at low potentials, besides displaying mixed proton–electron conductivity [12–14]. Such properties could give hydrous ruthenium oxide interesting properties, such as the ability to function as a co-catalyst for methanol oxidation [15–17].

The role of ruthenium atoms when combined with Pt on methanol oxidation is well established [5,9,18–20]. However, the role of hydrous oxide species still has to be investigated, so that more efficient materials can be obtained. Some works about the electrooxidation of organic molecules on Pt associated with metal oxides can be found in the literature [21–28], but the application of these materials as catalysts in DMFC is scarce [12,13,23,29,30].

In this work, Pt–RuO_2/C electrodes have been prepared by thermal decomposition of polymeric precursors and characterized by X-ray diffraction (XRD), transmission electron microscopy (TEM), and cyclic voltammetry (CV). Their electrocatalytic activity towards methanol oxidation has been verified in a single DMFC working with methanol solution.

2. Experimental

Several Pt–RuO_2 catalysts of different compositions (50, 60, 70, 80, and 100% Pt content) were prepared, by thermal decomposition of polymeric precursors [31]. The precursor solutions were prepared by dissolution of citric acid in ethyleneglycol, under stirring at 60 °C. The temperature was increased to 90 °C, after the full dissolution of citric acid, and either the H_2PtCl_6 or $RuCl_3$ solution (both 1:1, v/v HC1) was added. These solutions were prepared in a metal (Pt or Ru):citric acid:ethyleneglycol molar ratio of 1:4:16.

In order to obtain the catalyst supported on carbon powder for DMFC, the precursor solutions were mixed to high surface area carbon powder (Vulcan XC-72) in the desired proportion. They were sonicated for 1 h and further calcinated at 400 °C for 1 h. The final metal loading was 40 wt.%. In order to obtain non-supported catalysts for comparative studies, another catalyst was obtained without adding the carbon powder to the precursor solution. The solutions were mixed in an adequate proportion and calcinated at 400 °C. In this way, two kinds of catalysts were obtained: supported on carbon powder and non-supported.

The crystalline structures of the catalyst were studied by XRD performed on a SIEMENS D5005 diffractometer using a Cu Kα source. The X-ray diffractograms were obtained for 2θ values varying between 20° and 70°.

The mean sizes of the oxide particles were determined from the X-ray diffractograms, using the Scherer equation and assuming that the particles are spherical

$$L = 0.9\lambda / B_{2\theta} \cos\theta_{\max}$$

where λ is the X-ray wavelength (1.54056 Å for the Cu Kα radiation), $B_{2\theta}$ is the width of the diffraction peak at half-height, and $\theta_{\max}$ is the angle at the peak maximum position.

TEM analysis was performed on a Philips CM 120 equipment. Catalyst samples were suspended in alcohol, homogenized and deposited on a standard Cu grid covered with a carbon film. Catalyst morphology and chemical composition were investigated by scanning electronic microscopy (SEM) and energy dispersive X-ray (EDX) analysis, using a Zeiss DSM 940 microscope linked to a Link Analytical QX 2000 microanalyzer, with the samples immobilized on an Al support.

The surface features of the catalyst and their catalytic activity toward methanol oxidation were evaluated in half-cell experiments by cyclic voltammetry, using an Ecochemie Autolab PGSTAT20 potentiostat/galvanostat. All measurements were carried out at room temperature (22 °C), in a 0.5 mol L^{-1} H_2SO_4 solution, at 20 mV s^{-1}, using with a reversible hydrogen electrode (RHE) as reference and a Pt wire as the counter-electrode. The working electrode was prepared by ultrasonically mixing the catalyst with a solution containing Nafion® ionomer and isopropanol. After the suspension had been homogenized, a given volume of the catalyst solution was deposited onto a freshly-polished Au substrate, and the solvent was evaporated at room temperature. The metal loading on the formed catalyst layer was close to 0.07 mg cm^{-2}. The concentration of the methanol solution was 0.1 mol L^{-1}.

Preliminary tests were carried out in a single DMFC. Electrodes were prepared by applying the suspension on a PTFE/Vulcan XC-72 diffusion layer deposited onto a carbon cloth, followed by solvent evaporation at 50 °C. The final metal loading was 2.0 mg cm^{-2}. The cathode used in all DMFC measurements was 20% Pt/C from E-TEK.

Electrodes were hot pressed onto a purified Nafion® 117 membrane, at 130 °C, for 3 min. The electrode-membrane assembly with a 5 cm^2 geometric surface area was placed into a single cell, between carbon plates with channels to allow the flow of both oxygen/air and the methanol solution. The cell temperature at both the anode and cathode compartments was monitored by thermocouples. The cell was operated at 90 °C, with a 2.0 mol L^{-1} methanol solution flowing at 1.0 mL min^{-1}, and oxygen flowing at a 2.5 bar pressure controlled by a Globe Tech station.

3. Results and discussion

3.1. XRD analyses

Fig. 1 shows the X-ray diffractograms for Pt–RuO_2 catalysts supported on carbon (Fig. 1A) or non-supported (Fig. 1B). The peaks at $2\theta = 40°$, 47°, and 67° are associated to the (1 1 1), (2 0 0), and (2 2 0) planes of the fcc platinum structure, respectively. The peaks at $2\theta = 28°$, 35°, and 54° correspond to a crystalline material with rutile phase, attributed to RuO_2. Another peak at $2\theta = 44°$ can also be seen and may be associated to the presence of metallic Ru [15,32]. No peak due to Pt oxides species can be observed; only the formation of metallic Pt occurs. Comninellis and Vercesi [33,34] have shown that the formation of Pt with a high degree of crystallinity is favoured instead of its oxide, and this fact can be noted from the presence of high and narrow Pt peaks in the diffractograms. The ratio between the Pt and RuO_2 diffraction peaks is proportional to the contents of Pt and Ru. This can be attributed to the low amount of Ru in the oxide and to the low crystallinity of RuO_2. The calcination temperature used to prepare the catalysts (400 °C) favoured the

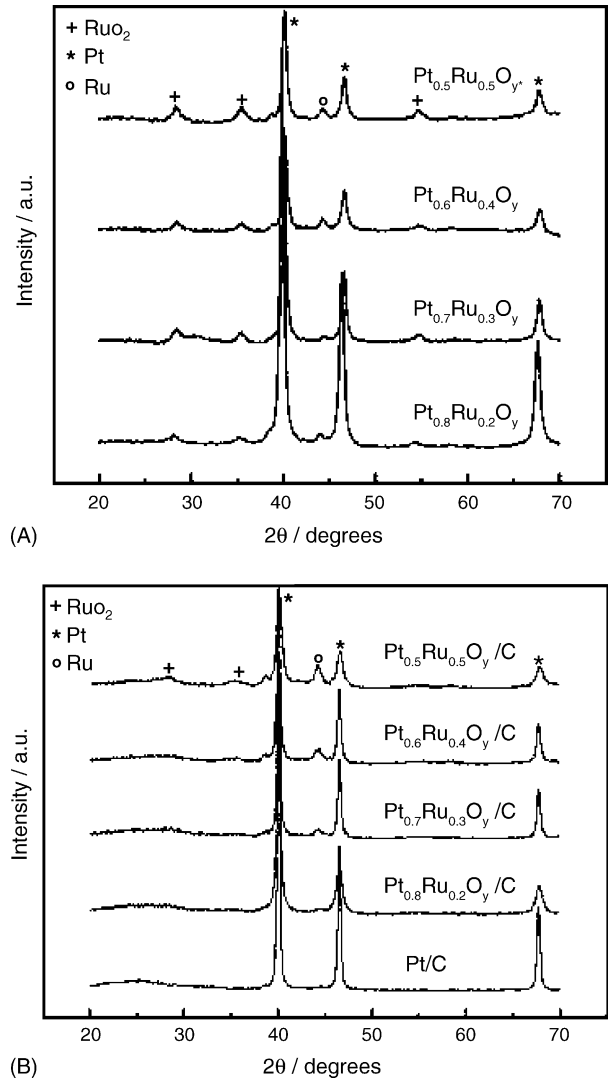

Fig. 1. X-ray diffraction patterns for Pt–RuO_2 catalysts: (A) non-supported and (B) supported on carbon powder substrate.

formation of a hydrous RuO_2 phase with low cristallinity, and only temperatures of ca. 500 °C yielded phases with high degree of crystallinity [15]. This hydration water within the RuO_2 structure gives the catalyst protonic conductivity properties as well as electronic conductivity, and such properties could increase the catalyst efficiency towards methanol oxidation [12,13].

The average particle size was calculated from X-ray diffractograms using the Pt diffraction peak at $2\theta = 40°$. Table 1 shows that values vary between 13 and 25 nm, with both the supported and non-supported catalysts. These values are high if compared to those obtained through other preparation methods described in the literature [15,16]. In this case, the thermal treatment provokes crystallization and crystal growth, thus increasing the particle size.

Table 1
Average Pt particle size determined by the Scherrer equation

Composition	Average particle size (nm)	
	$Pt_xRu_{(1-x)}O_y$	$Pt_xRu_{(1-x)}O_y/C$
$Pt_{0.5}Ru_{0.5}O_y$	15.6	13.4
$Pt_{0.6}Ru_{0.4}O_y$	15.9	24.2
$Pt_{0.7}Ru_{0.3}O_y$	18.0	25.6
$Pt_{0.8}Ru_{0.2}O_y$	16.2	13.8
$Pt_{1.0}O_y$	19.1	25.7

3.2. Morphology

Fig. 2 shows representative micrographs obtained by TEM for both the supported and non-supported catalysts. The non-supported catalysts (Fig. 2A) clearly form large agglomerates, whereas the metal particles are anchored on carbon and homogeneously distributed in the supported catalysts (Fig. 2B).

The morphological features were also investigated by SEM and there was substantial agreement with the TEM results. Fig. 3 shows a micrograph of the 80% Pt non-supported catalyst, where the presence of large agglomerates can be observed. Taking this catalyst as an example, the EDX analysis confirms that the overall composition (Pt = 76 and Ru = 24) is close to the nominal one. It is noteworthy that only the whole composition and not the surface one, can be known from EDX analysis. This homogeneous composition is due to the preparation method used in this work, which keeps the metal inside a polymeric chain, avoiding metal loss during the calcination processes [35]. Similar behavior had been observed in a previous work, where the catalysts were prepared on a Ti plate substrate using the same method above, ensuring that the polymeric precursor method led to uniform and homogeneous films with controlled stoichiometry, as well as high chemical and physical stability [36].

3.3. Electrochemical characterization of the catalysts

The electrocatalytic properties of the catalysts were investigated by cyclic voltammetry in a 0.5 mol L^{-1} H_2SO_4 solution, at 20 mV s^{-1}. Fig. 4 shows representative voltammograms of the non-supported mixed catalysts, which present a similar behavior to that of polycrystalline Pt with well-defined hydrogen adsorption/desorption peaks and Pt oxidation/reduction regions. Additionally, there is some process occurring in the double-layer region. This increase in current has been previously observed with Pt–RuO_2 catalysts [36,37], and it can be attributed to the transition between the Ru(III) and Ru(IV) oxidation states. Due to the existence of different Ru oxidation states in this potential range, ruthenium oxides are able to adsorb large amounts of OH species during the polarization process. They achieve varied metal oxidation states through a mechanism involving proton exchange with solution [38]

$$RuO_x(OH)_y + \delta e^- + \delta H^+ \leftrightharpoons RuO_{x-\delta}(OH)_{y+\delta}$$

The voltammetric behavior depends on the Pt content. As expected, better definition of the hydrogen peaks and smaller currents in the double-layer region are observed for a higher Pt content. In contrast, hydrogen peaks are not well-defined and currents in the double-layer region are higher in the case of lower amounts of Pt. Such increase in the double-layer currents indicates that the Ru sites are exposed to the solution, contributing to

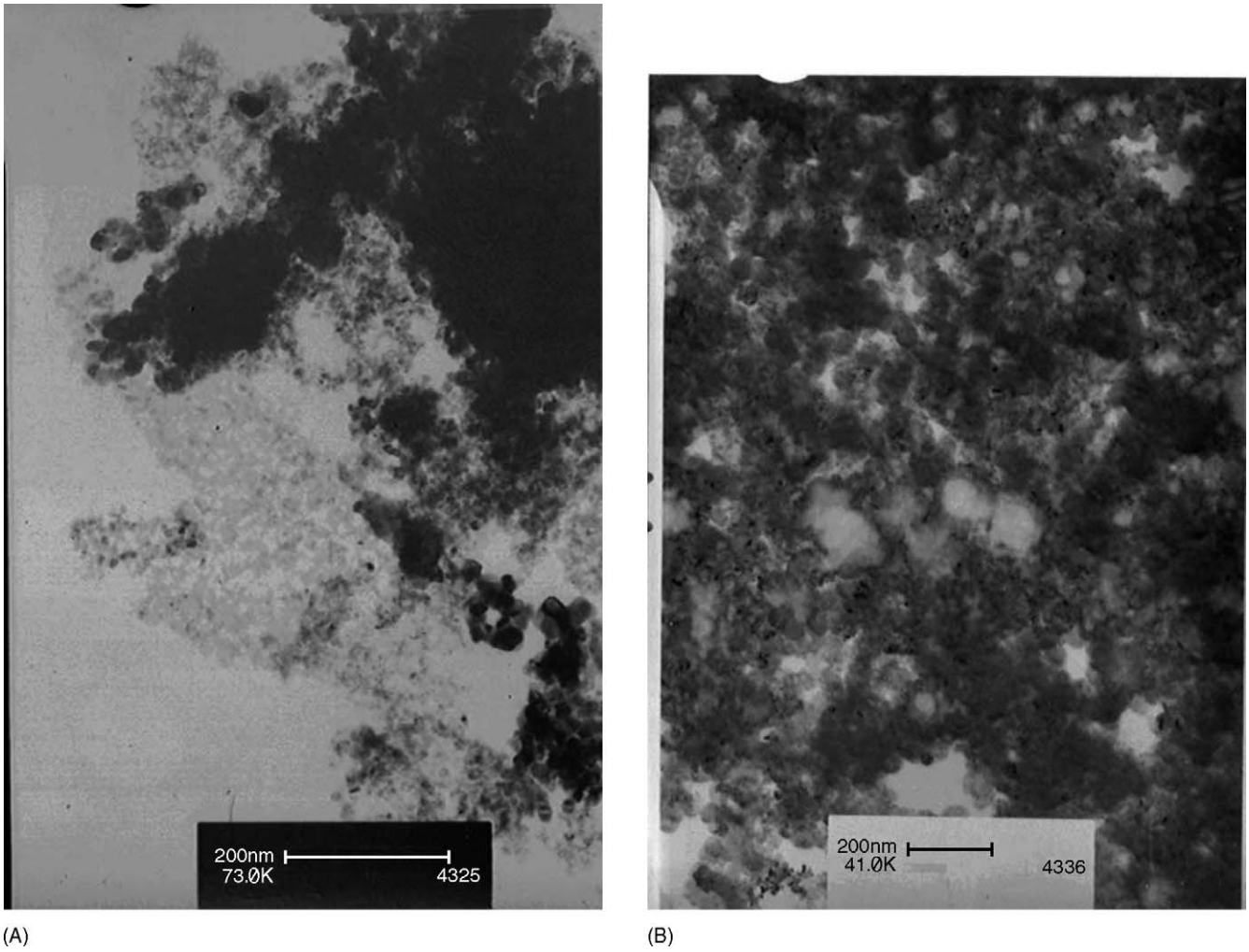

Fig. 2. TEM images of $Pt_{0.8}Ru_{0.2}O_y$ electrode containing: (A) non-supported catalysts and (B) catalysts supported on carbon powder.

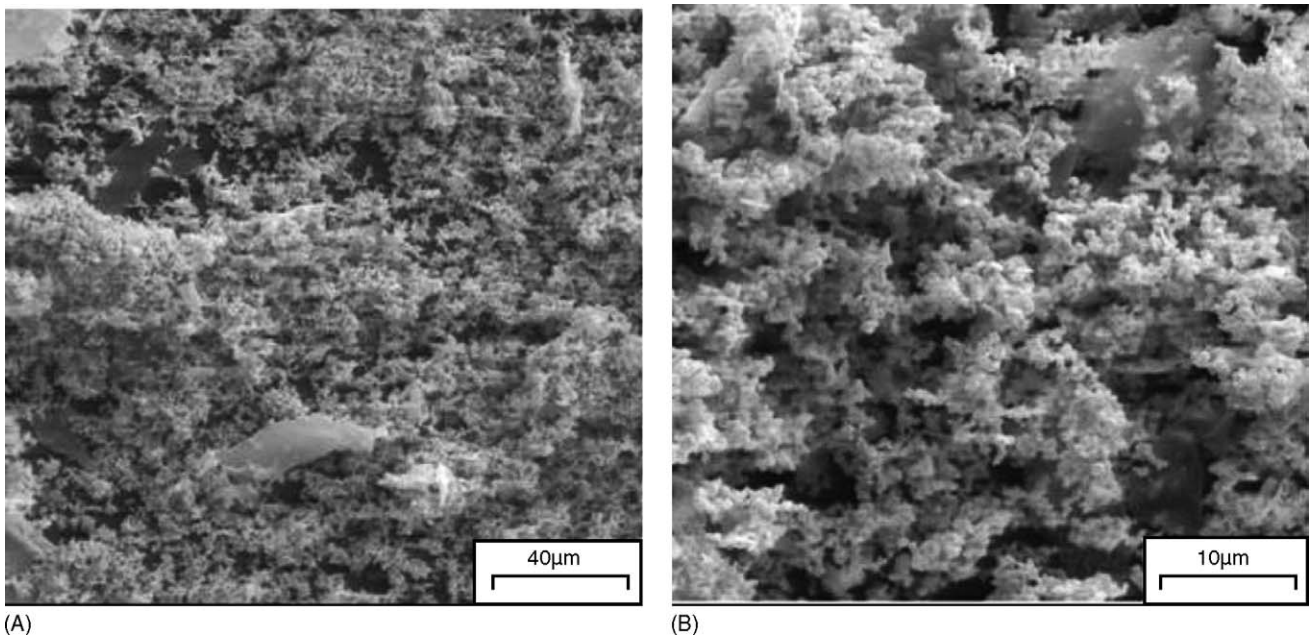

Fig. 3. SEM micrographs of $Pt_{0.8}Ru_{0.2}O_y$ electrode. (A) Amplification: 500× and (B) amplification: 2000×.

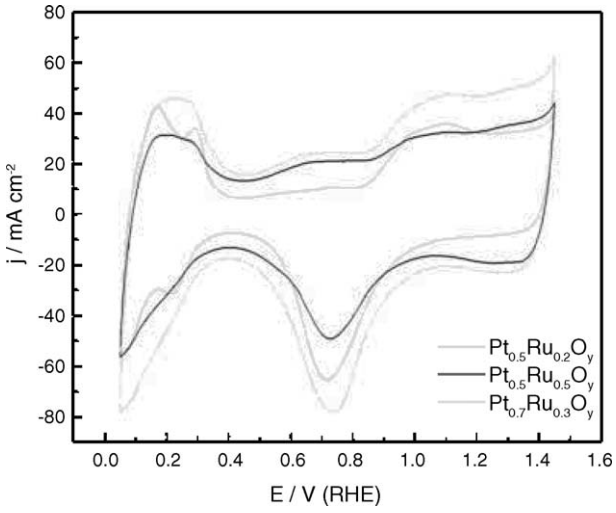

Fig. 4. Representative voltammograms at 20 mV s^{-1} of Pt–RuO_2 electrodes in a 0.5 mol L^{-1} H_2SO_4 solution.

the surface electrochemical behavior and to its ability to adsorb large quantities of OH species.

3.4. Methanol oxidation

In order to determine whether the catalyst is active toward methanol oxidation or not, cyclic voltammetry experiments were performed in a 0.1 mol L^{-1} methanol solution.

Fig. 5 shows the voltammetric behavior of the non-supported $Pt_{0.8}Ru_{0.2}O_y$ catalyst. For all the electrocatalysts tested, the current values in the hydrogen region decrease due to methanol adsorption. At potential values slightly more positive than the hydrogen desorption process, the oxidation currents increase until a maximum is reached at about 0.7 V. No peak due to methanol oxidation appears in the cyclic voltammogram of pure RuO_2 (without Pt).

Although electrode composition and particle dispersion have a significant electrocatalytic influence on the behavior toward

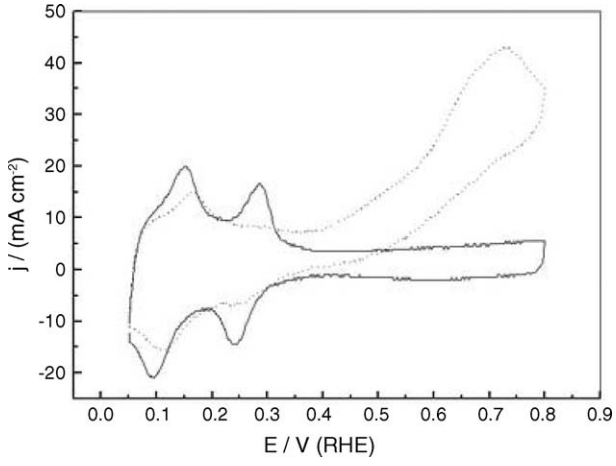

Fig. 5. Cyclic voltammogram of the $Pt_{0.8}Ru_{0.2}O_y$ electrode at 20 mV s^{-1} in a (—) 0.5 mol L^{-1} H_2SO_4 solution, and in a (- - -) 0.5 mol L^{-1} H_2SO_4 + 0.1 mol L^{-1} methanol solution.

Table 2
Maximum power density obtained for each catalyst at the respective current density

Electrode composition	$Pt_xRu_{(1-x)}O_y$		$Pt_xRu_{(1-x)}O_y$/C	
	mW cm^{-2}	mA cm^{-2}	mW cm^{-2}	mA cm^{-2}
$Pt_{1.0}O_y$	7.1	60	7.2	60
$Pt_{0.5}Ru_{0.5}O_y$	16.4	120	16.1	100
$Pt_{0.6}Ru_{0.4}O_y$	15.4	100	32.8	200
$Pt_{0.7}Ru_{0.3}O_y$	13.0	80	5.3	40
$Pt_{0.8}Ru_{0.2}O_y$	18.8	140	23.1	140

methanol oxidation, the general features of the voltammetric curves are similar for all catalysts, either non-supported or supported on carbon powder. This fact is better confirmed by preliminary experiments performed in a complete fuel cell.

Fig. 6 reports the cell voltage versus current density curves for both the non-supported (Fig. 6A) catalysts and the carbon supported catalysts (Fig. 6B), for various electrode compositions. Table 2 gives the maximum values of power density obtained at the respective current density for each catalyst.

Comparing the electrocatalytic activities of electrodes of different compositions, higher power densities are obtained for catalysts dispersed on carbon powder, mainly $Pt_{0.6}Ru_{0.4}O_y$/C, which leads to the highest value (~33 mW cm^{-2} at 200 mA cm^{-2}). Moreover, all mixed catalysts present better performance than that of the Pt electrode alone, indicating that RuO_2 has a crucial contribution toward methanol oxidation. Differences in the performance of the electrodes with different compositions are a consequence of several factors. It is important to remember that the current values are not normalized to the real surface area, but to the geometric area. This implies that the observed maximum may be due to (i) a better distribution of Ru in adjacent sites of Pt particles, which may increase the bifunctional mechanism, (ii) an enhancement in the Pt activity due to electronic effects, and (iii) an increase in the surface area available for occurrence of the adsorption process. The observed catalytic activity must be analyzed as an overall activity and not only as an intrinsic activity.

As expected, the catalytic activity is also dependent on particle dispersion. The performance of the catalysts prepared by dispersion on carbon powder is higher than that oft the non-supported materials, which can be attributed to better particle distribution on the carbon support. Despite the lower performance of the non-supported catalyst, a higher activity is observed for mixed catalysts when compared to Pt alone, suggesting that RuO_2 is necessary to achieve better electroactivity, as proposed by Rolison and co-workers [12,13].

Although a density value of 33 mW cm^{-2} was obtained with $Pt_{0.6}Ru_{0.4}O_y$/C, such value is considered to be too low for a DMFC [1,2]. Indeed, the low efficiency of the catalyst is due to the preparation method, which led to poor dispersion of the metallic particles on the carbon substrate, as seen in the previous micrographs (Figs. 2 and 3). Knowing that the electrocatalytic efficiency is related to the preparation conditions, the choice of the synthetic method must aim at good particle dispersion on the support, decreasing the particle size and thus increasing the

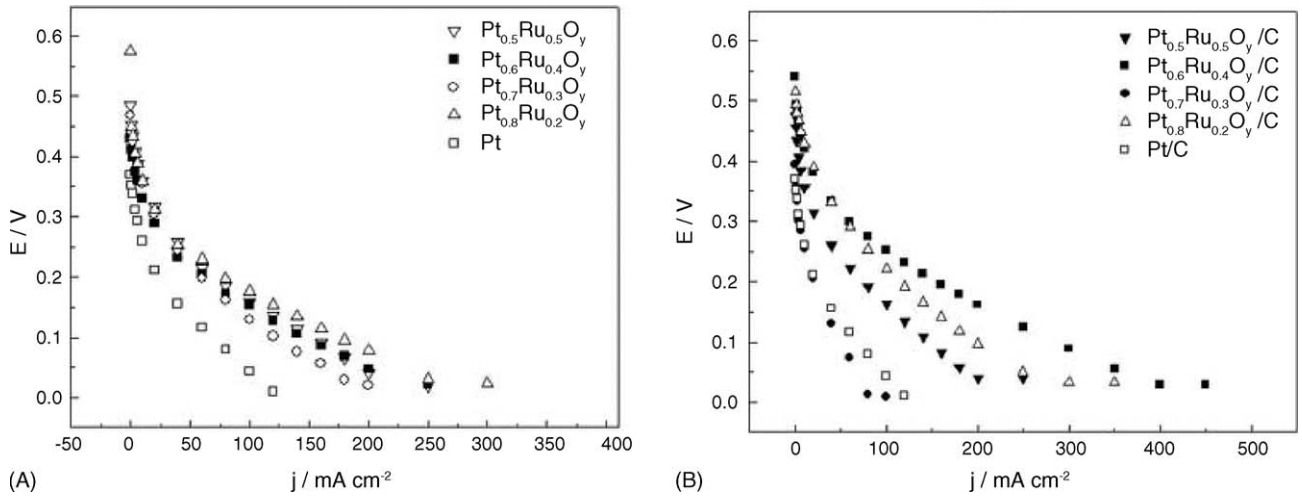

Fig. 6. *E* vs. *i* curves recorded in a single DMFC operating with a 2.0 mol L^{-1} methanol solution using: (A) non-supported catalysts and (B) catalysts supported on carbon powder.

real surface area and the number of catalytic sites necessary for the adsorption of OH species.

Further studies will be carried out by modifying the synthetic conditions, such as the annealing temperature and reagent concentration, in order to improve the method toward smaller particle sizes and better particle dispersion on the carbon powder.

4. Conclusion

In this work, the preparation and characterization of Pt–RuO_2 powder catalysts prepared by thermal decomposition of polymeric precursors has been reported. The synthetic method employed herein allowed the easy preparation of materials applicable to DMFC anodes.

Two kinds of catalysts were prepared, non-supported and supported on a carbon powder substrate. Both types presented structures recognized as being due to Pt and RuO_2 by XRD analysis, and controlled stoichiometry was confirmed by EDX analysis. Micrographs showed that the non-supported catalysts are arranged in large agglomerates, whereas the metallic particles are anchored on the carbon powder substrate in the supported catalysts.

Electrochemical measurements in half-cell and in a complete fuel cell showed the contribution of RuO_2 toward methanol oxidation. Different electrode performance as a function of catalyst composition and dispersion was observed. The best power density (33 mW cm^{-2} at 200 mA cm^{-2}) was obtained with the $Pt_{0.6}Ru_{0.4}O_y$/C electrode.

Even though the synthetic method proposed in this preliminary study did not greatly improve the catalytic activity, results indicate that the thermal decomposition of polymeric precursors is a promising route for the production of catalysts supported on carbon powder applicable to DMFC. The improvement of the catalytic activity may be obtained by changing the calcination parameters like temperature and calcination time. Another way to improve material performance is to optimize the composition of the precursor solution. These investigations are currently being carried out in our laboratory.

Acknowledgments

The authors thank FAPESP, CAPES and COFECUB for financial support.

References

[1] C. Lamy, A. Lima, V. LeRhun, F. Delime, C. Coutanceau, J.-M. Léger, J. Power Sources 105 (2002) 283–296.
[2] K. Scott, W.M. Taama, P. Argyropoulos, J. Power Sources 79 (1999) 43–59.
[3] H. Wendt, M. Linardi, E.M. Aricó, Quim. Nova 25 (2002) 470–476.
[4] T. Iwasita, Electrochim. Acta 47 (2002) 3663–3674.
[5] W.F. Lin, T. Iwasita, W. Vielstich, J. Phys. Chem. 103 (1999) 3250–3257.
[6] H.A. Gasteiger, N. Markovic, P.N. Ross, E.J. Cairns, J. Phys. Chem. 98 (1994) 617–625.
[7] H.A. Gasteiger, N. Markovic, P.N. Ross, E.J. Cairns, Electrochim. Acta 39 (1994) 1825–1832.
[8] M.D. Spasojevic, R.R. Adzic, A.R. Despic, J. Electroanal. Chem. 109 (1980) 261–269.
[9] M. Watanabe, S. Motoo, J. Electroanal. Chem. 60 (1975) 267–273.
[10] G. Tremiliosi-Filho, H. Kim, W. Chrzanowski, A. Wieckowski, B. Grzybowska, P. Kulesza, J. Electroanal. Chem. 467 (1999) 143–156.
[11] P. Waszczuk, G.-Q. Lu, A. Wieckowski, C. Lu, C. Rice, R.I. Masel, Electrochim. Acta 47 (2002) 3637–3652.
[12] J.W. Long, R.M. Stroud, K.E.S. Lyons, D.R. Rolison, J. Phys. Chem. B 104 (2000) 9772–9776.
[13] D.R. Rolison, P.L. Hagans, K.E. Swider, J.W. Long, Langmuir 15 (1999) 774–779.
[14] K.-W. Park, Y.-E. Sung, J. Appl. Phys. 94 (2003) 7276–7280.
[15] K. Lasch, L. Jorissen, K.A. Friedrich, J. Garche, J. Solid State Electrochem. 7 (2003) 619–625.
[16] K. Lasch, G. Hayan, L. Jorissen, J. Garche, O. Besenhardt, J. Power Sources 105 (2002) 305–310.
[17] H.B. Suffredini, V. Tricoli, L.A. Avaca, N. Vatistas, Electrochem. Commun. 6 (2004) 1025–1028.
[18] T. Iwasita, H. Hoster, A. John-Anacker, W.F. Lin, W. Vielstich, Langmuir 16 (2000) 522–529.
[19] T. Iwasita, J. Braz. Chem. Soc. 13 (2002) 401–409.
[20] J.M. Léger, Electrochim. Acta 50 (2005) 3123–3129.

[21] J.H. White, A.F. Sammells, J. Electrochem. Soc. 140 (1993) 2167–2177.
[22] L.D. Burke, O.J. Murphy, J. Electroanal. Chem. 101 (1979) 351–361.
[23] P.C. Biswas, T. Ohmori, M. Enyo, J. Electroanal. Chem. 305 (1991) 205–215.
[24] T. Ohmori, Y. Nodasaka, M. Enyo, J. Electroanal. Chem. 281 (1990) 331–337.
[25] A. Katayama, J. Phys. Chem. 84 (1980) 376–381.
[26] E.J.M. O'Sullivan, J.R. White, J. Electrochem. Soc. 136 (1989) 2576–2583.
[27] A. Aramata, I. Toyoshima, M. Enyo, Electrochim. Acta 37 (1992) 1317–1320.
[28] G. Fóti, D. Gandini, Ch. Comninellis, A. Perret, W. Haenni, Electrochem. Sol. State Lett. 2 (1999) 228–230.
[29] L.X. Yang, R.G. Allen, K. Scott, P.A. Christenson, S. Roy, J. Power Sources 137 (2004) 257–263.
[30] L.X. Yang, RG. Allen, K. Scott, P.A. Christenson, S. Roy, Electrochim. Acta 50 (2005) 1217–1223.
[31] M. P. Pechini, S. Adams, US Patent 3,330,697 (1967).
[32] F. Colmati Jr., W.H. Lizcano-Valbuena, G.A. Câmara, E.A. Ticianelli, E.R. Gonzalez, J. Braz. Chem. Soc. 13 (2002) 474–482.
[33] Ch. Comninellis, G.P. Vercesi, J. Appl. Electrochem. 21 (1991) 335–345.
[34] Ch. Comninellis, G.P. Vercesi, J. Appl. Electrochem. 21 (1991) 136–142.
[35] E.C.P.E. Rodrigues, P. Olivi, J. Phys. Chem. Solids 64 (2003) 1105–1112.
[36] M.B. Oliveira, L.P.R. Profeti, P. Olivi, Electrochem. Commun. 7 (2005) 703–709.
[37] C.-C. Hu, C.-H. Lee, T.-C. Wen, J. Appl. Electrochem. 26 (1996) 72–82.
[38] S. Trasatti, Electrochim. Acta 36 (1991) 225–241.